

# Preparation and characterization of doped WO<sub>3</sub> photocatalyst powders

M. ASHOKKUMAR, P. MARUTHAMUTHU\*

Department of Energy, University of Madras, A.C. College Campus, Madras 600 025, India

WO<sub>3</sub> semiconductor particles, useful in solar energy conversion processes, were doped with transition metal ions, Ti(III), V(IV), Cr(III), Mn(II), Fe(III), Co(II), Ni(II), Cu(II), Zn(II) and Ru(III) by a high-temperature sintering technique. The method of preparation of these photocatalysts is described in detail. The structural changes effected during sintering were investigated by X-ray powder diffraction (XRD) and scanning electron microscopy (SEM). The XRD analysis indicated that the monoclinic crystal structure of WO<sub>3</sub> was not altered during sintering. SEM studies showed that the sizes of the particles ranged from 1 to 10 μm and the crystallinity was increased due to doping. The dopants were found to be mostly distributed on the surface of WO<sub>3</sub> particles.

## 1. Introduction

WO<sub>3</sub> semiconductor powders have been used for solar energy conversion processes by many researchers. Oxygen generation [1, 2] from water, synthesis of amino acid [3, 4] and water photolysis into hydrogen and oxygen [5] are some of the works reported using this semiconductor. The absorbance in the visible region [6] and photocatalytic activities [7] of WO<sub>3</sub> powders were found to be increased by doping with transition metal ions. Doping is usually done by sintering at high temperatures. Photosynthetic deposition of copper on TiO<sub>2</sub> and WO<sub>3</sub> powders was carried out by Reiche *et al.* [8] and photoelectrolytic deposition of platinum was reported by Curran *et al.* [9]. Photo-assisted platinum deposition using platinum complexes was done by Hermann *et al.* [10]. Physical characterizations of the semiconductor materials are usually determined by diffuse reflectance measurements [6], X-ray diffraction (XRD) [11] and scanning electron microscopy (SEM) [12].

In this paper, we report for the first time, the preparation and characterization of doped WO<sub>3</sub> powders. Doping with transition metal ions was done by sintering at high temperature. The photocatalysts prepared were characterized using powder X-ray diffraction and scanning electron microscopy. This study was carried out to determine (i) the change in the crystal structure, (ii) the surface modifications, (iii) the change in the particle sizes, and (iv) the change in the surface area, effected due to doping by a high-temperature sintering technique, because these properties play very important roles in the photocatalytic efficiencies of these semiconductor powders towards solar energy conversion.

## 2. Experimental procedure

### 2.1. Preparation of the photocatalysts

WO<sub>3</sub> used was obtained from Fluka (Fluka, Switzerland) (>99.99%) and the other chemicals used for

doping were of research grade and were used either as chlorides (TiCl<sub>3</sub>, CrCl<sub>3</sub>, MnCl<sub>2</sub>, FeCl<sub>3</sub>, RuCl<sub>3</sub>) or sulphates (VOSO<sub>4</sub>, CoSO<sub>4</sub>, NiSO<sub>4</sub>, CuSO<sub>4</sub>). Calculated amounts of transition metal compounds (containing ~4.0 at % metal ions) were mixed with weighed amounts of WO<sub>3</sub> to which 50 ml doubly distilled water was added and the contents were magnetically stirred for about 2 h to distribute the metal ions throughout the WO<sub>3</sub> particles. Then the water was evaporated by keeping the contents in an oven. The dried sample was ground to a powder, loaded into a silica boat and introduced into a tubular furnace. The temperature of the furnace was slowly raised to 800°C in an argon atmosphere and maintained at 800°C for 1 h. Then the temperature was maintained at 850°C for 2 h and 900°C for 1 h with stepwise increase in temperature. After sintering, the sample was cooled to room temperature and ground to powder.

### 2.2. Characterization techniques

X-ray diffraction measurements for the powders were taken with computer-controlled XRD units (X-ray generator PW 1130, Vertical Diffractometer PW 1050, Diffractometer Control Unit PW 1710; Philips, Holland). A copper target with a nickel filter was used (CuKα radiation; λ = 0.154 18 nm).

Scanning electron micrographs of the photocatalysts were taken using a Jeol JSM-35 CF Model with ×5000 magnification. The surface areas of these photocatalysts were determined by the BET method.

## 3. Results and discussion

### 3.1. XRD

X-ray powder diffraction measurements were taken with 2θ = 10° to 90° for undoped and Cu(II)-doped WO<sub>3</sub> powders. The 2θ values and the corresponding intensities of the peaks are shown in the spectra. The *d*-spacings and the corresponding *I*/*I*<sub>0</sub> values are given in Table I. Figs 1a and b show the XRD spectral

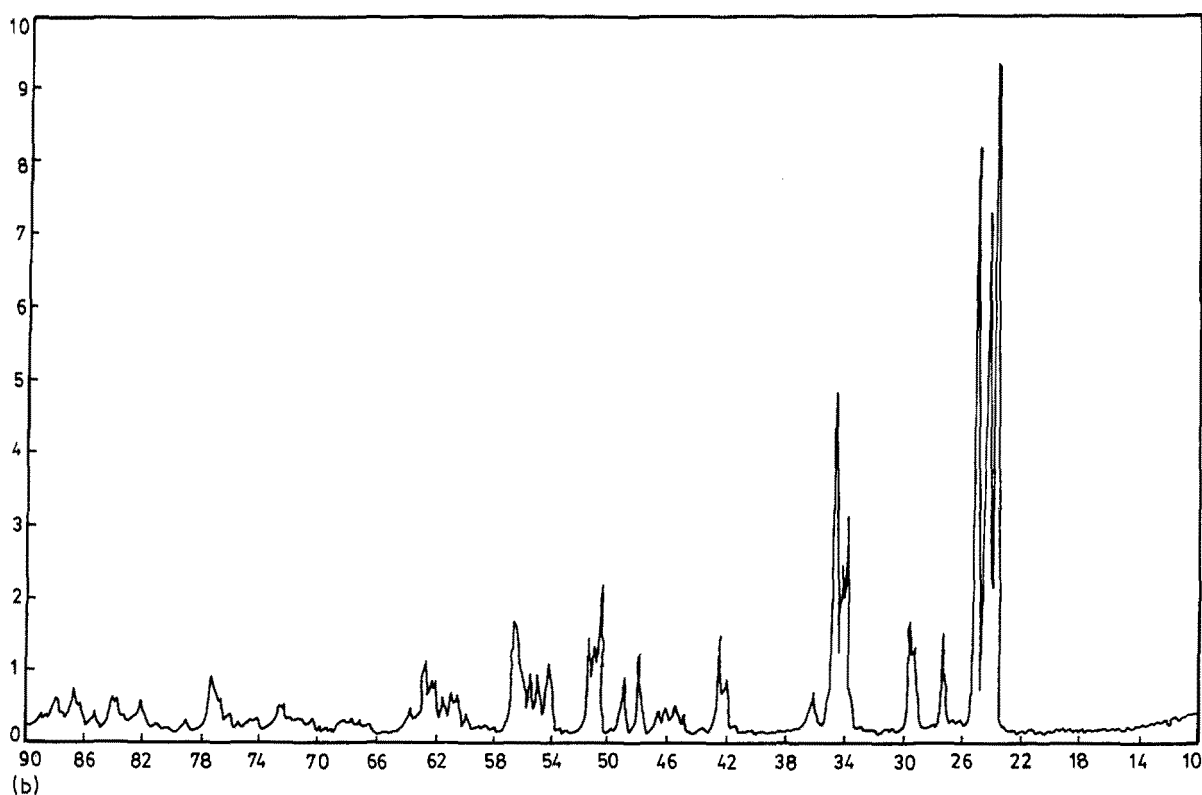
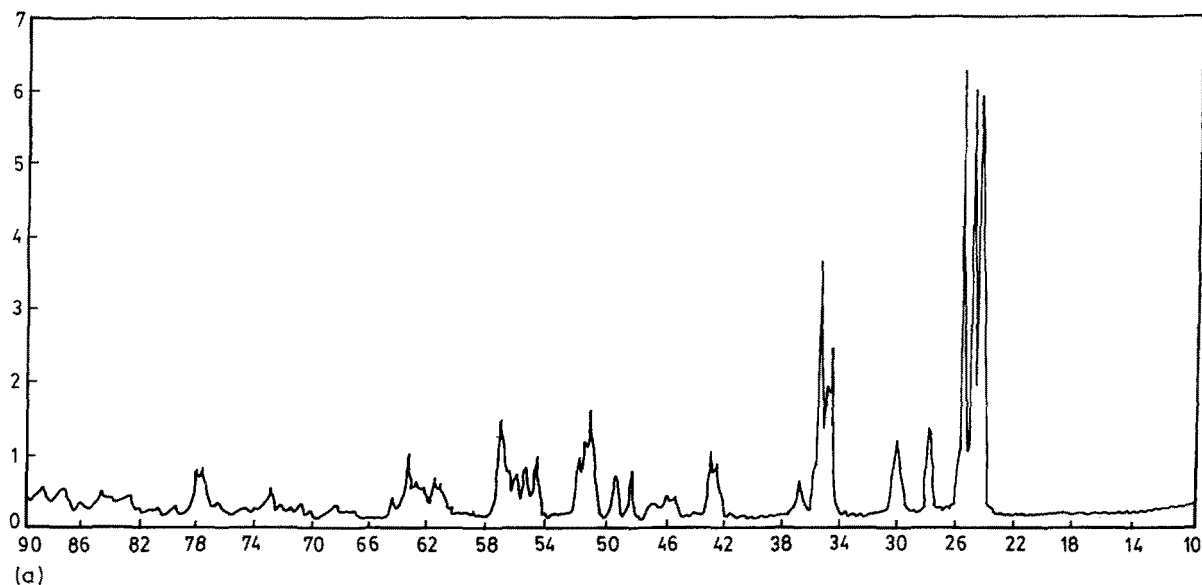


Figure 1 XRD spectrum of (a) undoped  $\text{WO}_3$  powders, (b) Cu(II)-doped  $\text{WO}_3$  powders (at % Cu  $\approx$  4.0).

observations for undoped and Cu(II)-doped  $\text{WO}_3$  powders, respectively. The  $2\theta$  values at which the major peaks appear are found to be almost the same for both the undoped and doped samples.

The observed differences in the intensities of the peaks may be due to the alteration of crystallinity on sintering. At the same time, sintering does not alter the crystal structure, which is proved by the  $d$ -spacing values observed. It is very interesting to note that the crystallinity of  $\text{WO}_3$  powders is increased due to doping as is evidenced from the observed more intense peaks in the spectrum (Fig. 1b) of the Cu(II)-doped  $\text{WO}_3$  sample. In Table I the  $d$ -spacings corresponding to the  $2\theta$  and  $I/I_0$  were given for undoped and Cu(II)-

doped  $\text{WO}_3$  along with the ASTM reported values for  $\text{WO}_3$  [13].

Comparing the observed  $d$ -spacings with those of ASTM, it is clear that they are almost the same in both cases. Hence, it is concluded that the crystal structure is not altered due to doping by the sintering technique. It is known that  $\text{WO}_3$  at room temperature has a monoclinic crystal structure [14]. Considering the above observations and discussions, the monoclinic crystal structure (end-centred) of  $\text{WO}_3$  is schematically shown in Fig. 2, where the corners have been occupied by oxygen atoms. The end faces of the crystal units (see Fig. 2) are occupied by tungsten and oxygen atoms, alternatively. It is also known that  $\text{WO}_3$  has a

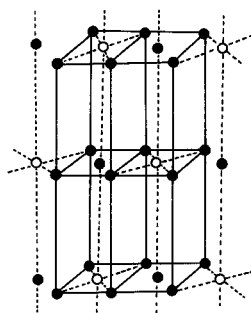


Figure 2 End-centred monoclinic crystal structure of  $\text{WO}_3$ . (○) W, (●) O. Each tungsten atom is surrounded by 6 oxygen atoms in a distorted “Oh” symmetry.

distorted octahedral (“Oh”) symmetry [14]. This is also shown in Fig. 2, where each tungsten atom is surrounded by six oxygen atoms in a distorted “Oh” symmetry.

However, it should be noted that the characteristic peaks of the dopant ions are not observed in the XRD spectrum (Fig. 1b) of  $\text{Cu(II)/WO}_3$ , i.e. there is no new  $d$ -value observed in the spectrum of the doped  $\text{WO}_3$  (Table I). This is due to the fact that a minimum of 10% concentration of the impurity ions is needed to effect their characteristic XRD peaks. However, only  $\sim 4\%$  concentrations were used here. It is also not clear whether the dopants are present as ions or oxides within the  $\text{WO}_3$  lattices. XRD study clearly illustrated that there is no change in the crystal structure of  $\text{WO}_3$  due to doping and proved that  $\text{WO}_3$  is present only as a trioxide and not as mixed oxides of tungsten.

Similar results reported on anatase by St John *et al.* [15], that the anatase structure was maintained even after reduction, support our observations on  $\text{WO}_3$ .

TABLE I XRD data

Reported, $\text{WO}_3$		Observed			
$d$ (nm)	$I/I_0$	$\text{WO}_3$ (Fluka)		$\text{WO}_3$ (doped)	
		$d$ (nm)	$I/I_0$	$d$ (nm)	$I/I_0$
0.3835	100	0.38070	99	0.38247	100
0.3762	95	0.37299	100	0.37472	78
0.3642	100	0.36203	82	0.36367	73
0.3342	50	0.33201	21	0.33330	15
0.3076	50	0.30776	15	0.30840	13
0.2684	75	0.26682	36	0.26827	28
0.2617	90	0.26080	53	0.26170	50
0.2149	60	0.21596	10	0.21515	14
0.1917	50	0.19145	13	0.19186	12
0.1879	50	0.18751	10	0.18803	10
0.1820	75	0.18177	25	0.18232	23
0.1793	50	0.17930	12	0.17953	11
0.1707	60	0.17070	15	0.17099	11
0.1687	55	0.16861	11	0.16894	9
0.1670	50	0.16674	9	0.16723	9
0.1638	65	0.16395	19	0.16414	15
0.1486	60	0.14862	14	0.14892	9
0.1242	20	0.12402	9	0.12406	9

### 3.2. SEM

Scanning electron micrographs were taken for all the photocatalysts prepared. Figs 3a to n show the photographs of these powders. The particle structures are found to be quite irregular. Most of the particles have monoclinic appearance. The irregularities in the particle structures might have occurred during grinding the samples at the time of preparation. Figs 3l, m and n are found to be useful in understanding the monoclinic crystal structure. The dopant ions are seen on the surfaces of the  $\text{WO}_3$  particles as minute white dots.

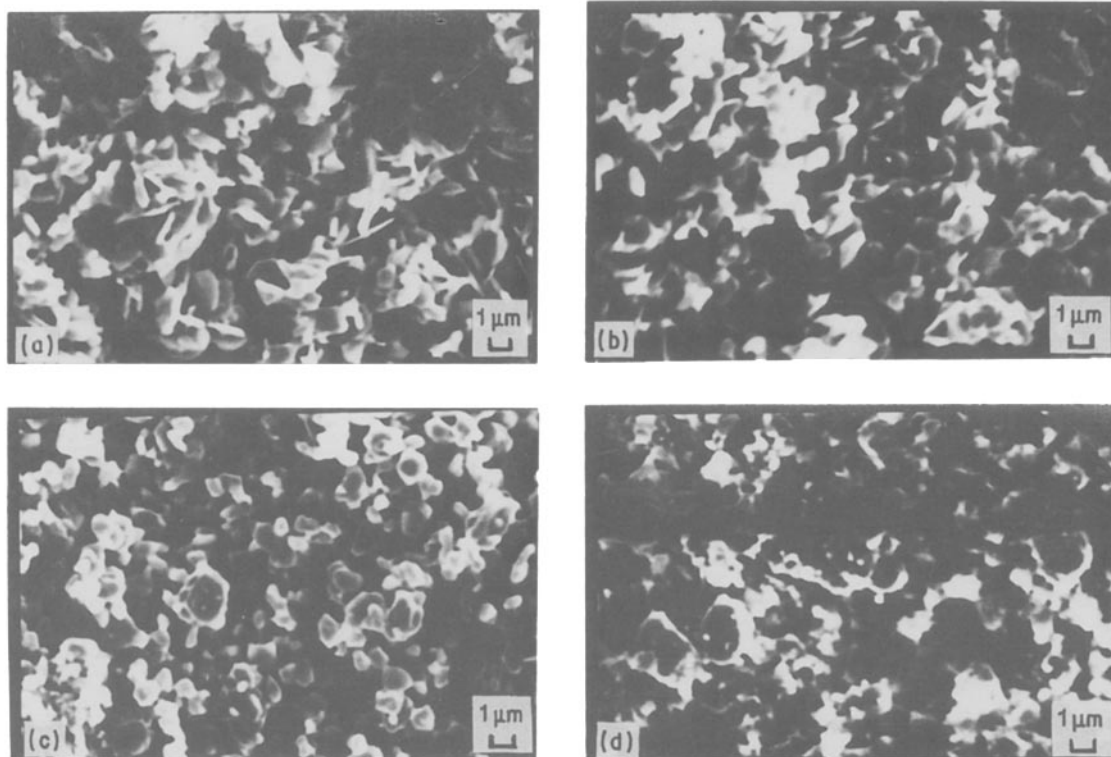


Figure 3 Scanning electron micrographs of: (a)  $\text{WO}_3$ , unprocessed; (b)  $\text{WO}_3$ , processed; (c)  $\text{Ti(III)/WO}_3$ ; (d)  $\text{V(IV)/WO}_3$ ; (e)  $\text{V}_2\text{O}_5/\text{WO}_3$ ; (f)  $\text{Cr(III)/WO}_3$ ; (g)  $\text{Mn(II)/WO}_3$ ; (h)  $\text{Fe(III)/WO}_3$ ; (i)  $\text{Co(II)/WO}_3$ ; (j)  $\text{Ni(II)/WO}_3$ ; (k)  $\text{Cu(II)/WO}_3$ ; (l)  $\text{Zn(II)/WO}_3$ ; (m)  $\text{RuO}_2$  (2.5%)/ $\text{WO}_3$ ; (n)  $\text{RuO}_2$  (7.5%)/ $\text{WO}_3$ .

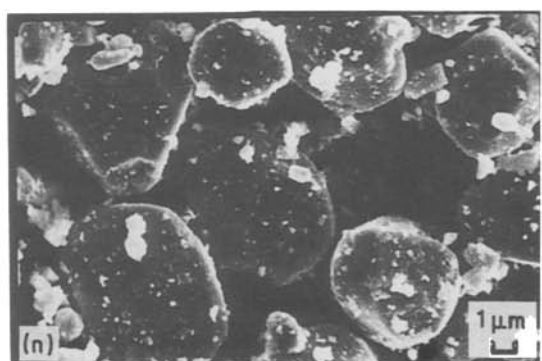
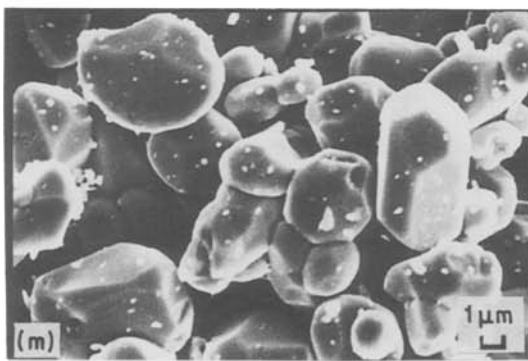
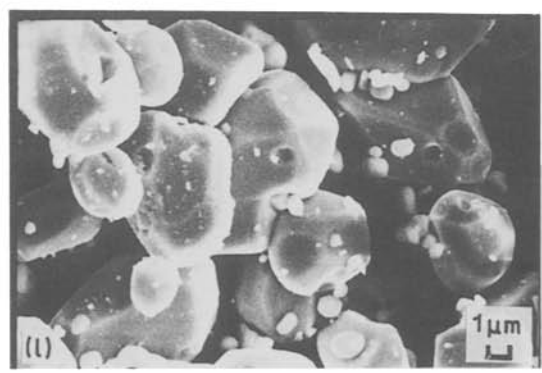
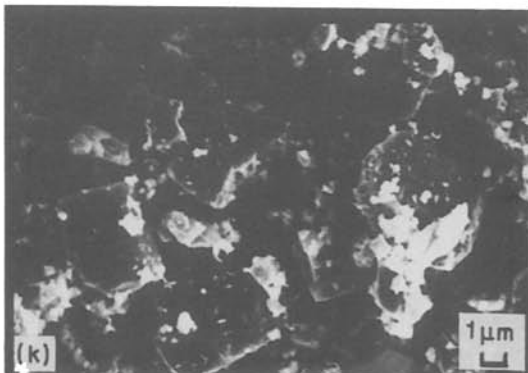
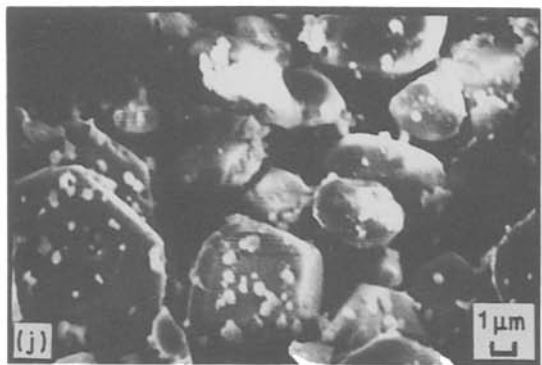
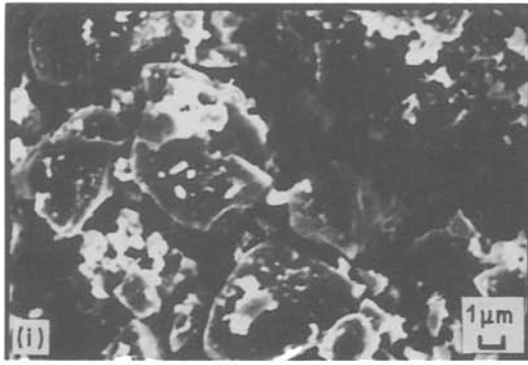
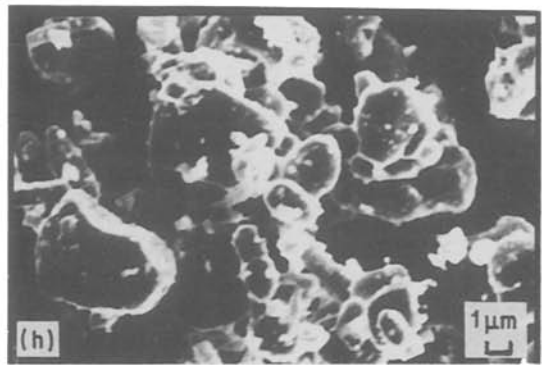
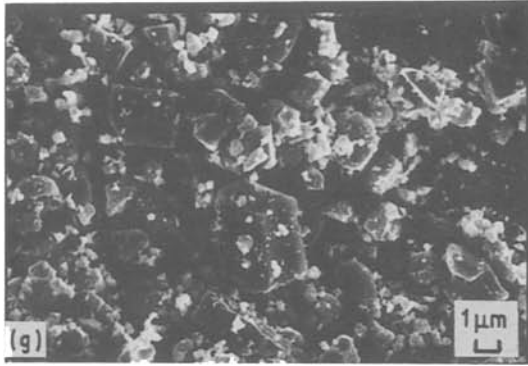
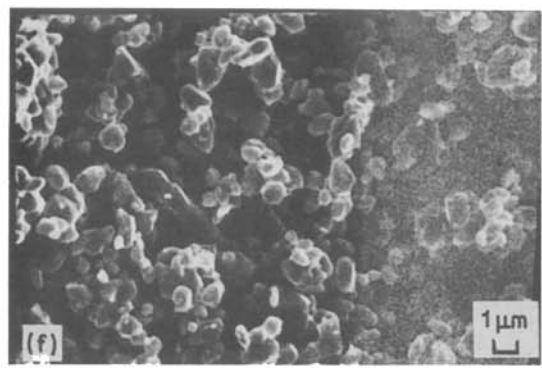
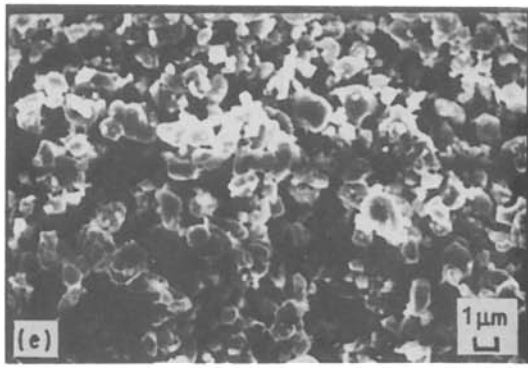


Figure 3 Continued.

However, there is every possibility for these dopants to occupy the interstitial positions, i.e. inside the unit lattices of  $\text{WO}_3$  particles. Moreover, it is also very clear from Figs 3g to n that the crystallinity is increased due to doping, which is indicated by the increase in particle (crystal) sizes with well-developed faces. The XRD spectra (Figs 1a and b), where we observe more intense and more sharp peaks in the case of doped sample (Fig. 1b), also support this.

The SEM particles also indicated that the particle sizes range from 1 to  $10\ \mu\text{m}$ . In Fig. 3a, because the particle sizes are very small, we observe more void spaces; whereas in the doped samples we observe larger particles with fewer void spaces. Austin Suthanthiraraj *et al.* [16] reported that as the grain sizes increase, which will result in a decrease in the number of void spaces, the conductivity of the material will be increased. Thus, due to sintering, the conductivity of the  $\text{WO}_3$  semiconductors could have been increased. The surface area of the undoped  $\text{WO}_3$  powders determined by the BET method is found to be  $\sim 1.5\ \text{m}^2\ \text{g}^{-1}$ . The surface areas of doped samples are in the range  $1.0$  to  $1.5\ \text{m}^2\ \text{g}^{-1}$ . The increase in the particles sizes are evinced from the micrographs has resulted in a decrease of the surface area of some of the doped samples from the values of the undoped ones. As the dopant concentration is increased from 2.5% (Fig. 1m) to 7.5% (Fig. 1n), the white dots appeared more densely in the micrograph picture (Fig. 1n), which illustrates that the dopants are mostly deposited on the surfaces.

#### 4. Conclusion

The  $\text{WO}_3$  semiconductor powders which are used for solar energy conversion processes were photosensitized by doping with transition metal ions. XRD and SEM techniques were used to characterize these materials. The dopants were found to be mostly distributed on the surface of  $\text{WO}_3$  particles. The surface areas of the doped  $\text{WO}_3$  are found to be less than those of the undoped  $\text{WO}_3$  with a consequent increase in the particle size of the former.

#### Acknowledgements

The authors thank Dr K. I. Vasu, Director, and his

research group, Central Electrochemical Research Institute, Karaikudi, India, Professor C. S. Swamy, Mr Varadhachary and Mr Krystopher, IIT, Madras, for their kind help in taking SEM, XRD and surface area measurements. One of the authors (M.A.) acknowledges the award of a Senior Research Fellowship by the University Grants Commission, New Delhi, India.

#### References

1. W. ERBS, J. DESILVESTRO, E. BORGARELLO and M. GRATZEL, *J. Phys. Chem.* **88** (1984) 4001.
2. J. DESILVESTRO and M. H. SPALLART, *J. Phys. Chem.* **89** (1985) 3684.
3. H. REICHE and A. J. BARD, *J. Amer. Chem. Soc.* **101** (1979) 3127.
4. W. W. DUNN, Y. AIKAWA and A. J. BARD, *ibid.* **103** (1981) 6893.
5. K. TENNAKONE and S. WICKRAMANAYAKE, *J. Chem. Soc. Faraday Trans.* **2** **82** (1986) 1475.
6. P. MARUTHAMUTHU and M. ASHOKKUMAR, *Sol. En. Mater.* **17** (1988) 433.
7. P. MARUTHAMUTHU and M. ASHOKKUMAR, *Int. J. Hydrogen Energy*, **13** (1988) 677.
8. H. REICHE, W. W. DUNN and A. J. BARD, *J. Phys. Chem.* **83** (1979) 2248.
9. J. S. CURRAN, J. DOMENECH, N. JAFFREZIC-RENAULT and R. PHILIPPE, *ibid.* **89** (1985) 957.
10. J. M. HERRMANN, J. DISDIER and P. PICHAT, *ibid.* **90** (1986) 6028.
11. B. REZIG, J. BOUGNOT, M. EL HAMMOUTI, M. PEROTIN VU BAY and M. SAVELLI, *Sol. En. Mater.* **9** (1983) 189.
12. T. HASE, B. W. LIN, T. ISEKI and H. SUZUKI, *J. Mater. Sci. Lett.* **5** (1986) 69.
13. "Powder Diffraction File", Inorganic Volume no. PDIS-5iRB, File No. 5-0363 and 5-0364 (The Joint Committee on Powder Diffraction Standards, Pennsylvania, 1960) p. 611.
14. J. C. BAILAR, H. J. EMELEUS, Sir RONALD NYHLON and A. F. TROTMAN-DICKENSON (eds), "Comprehensive Inorganic Chemistry", Vol. 3 (Pergamon, Oxford, 1973) p. 763.
15. M. R. ST JOHN, A. J. FURGALA and A. F. SAMMELLS, *J. Phys. Chem.* **87** (1983) 801.
16. S. AUSTIN SUTHANTHIRARAJ, S. RADHAKRISHNA and B. V. R. CHOWDRI, *J. Mater. Sci.* **19** (1984) 2863.

Received 29 March

and accepted 5 September 1988